Vol 18 No 10, October 2009
1674-1056/2009/18(10)/4541–06

Chinese Physics B

© 2009 Chin. Phys. Soc.
and IOP Publishing Ltd

Distribution of carriers in gradient-doping transmission-mode GaAs photocathodes grown by molecular beam epitaxy*

Zhang Yi-Jun(张益军), Chang Ben-Kang(常本康)†, Yang Zhi(杨 智), Niu Jun(牛 军), and Zou Ji-Jun(邹继军)

Institute of Electronic Engineering and Optoelectronic Technology, Nanjing University of Science and Technology, Nanjing 210094, *China*

(Received 11 January 2009; revised manuscript received 7 April 2009)

The gradient-doping structure is first applied to prepare the transmission-mode GaAs photocathode and the integral sensitivity of the sealed image tube achieves 1420 μA/lm. This paper studies the inner carrier concentration distribution of the gradient-doping transmission-mode GaAs photocathode after molecular beam epitaxy (MBE) growth using the electrochemical capacitance-voltage profiling. The results show that an ideal gradient-doping structure can be obtained by using MBE growth. The total band-bending energy in the gradient-doping GaAs active-layer with doping concentration ranging from 1×10^{19} cm^{-3} to 1×10^{18} cm^{-3} is calculated to be 46.3 meV, which helps to improve the photoexcited electrons movement toward surface for the thin epilayer. In addition, by analysis of the band offsets, it is found that the worse carrier concentration discrepancy between GaAs and GaAlAs causes a lower back interface electron potential barrier which decreases the amount of high-energy photoelectrons and affects the short-wave response.

Keywords: GaAs photocathode, gradient doping, molecular beam epitaxy, carrier concentration distribution

PACC: 7960, 7280E, 7320A

1. Introduction

Negative electron affinity (NEA) GaAs photocathodes activated by the coadsorption of cesium and oxygen have already found widespread application in modern night vision image intensifiers.[1−3] The GaAs photocathodes have been typically grown by metal-organic chemical vapor deposition (MOCVD) and molecular beam epitaxy (MBE).[4,5] The MOCVD technique is widely used due to its fast growth velocity and high throughput, whereas the MBE technique offers a precise control over the epilayer thickness and doping concentration level, which provides superior epitaxial quality. In the MBE growth of p-type GaAs photocathodes, the element beryllium (Be) is expected to be a suitable acceptor impurity for heavy doping and steep impurity profiles, because of its unique characteristics, such as near-unity sticking coefficient, low vapor pressure and high solubility in GaAs.[6]

Photoemission from GaAs NEA photocathodes is described as a three-step process of optical absorption, electron transport to the surface, and escape across the surface into vacuum.[7] In order to improve the performance of GaAs NEA photocathodes, such as electron diffusion length and surface electron escape probability, a gradient-doping structure on reflection-mode GaAs photocathodes was put forward,[8,9] which can obtain higher quantum efficiency than the uniform-doping one. However, there are few reports concerning the gradient-doping transmission-mode photocathodes. In this paper, we first apply this gradient-doping structure to prepare the transmission-mode GaAs photocathodes. In order to know the inner actual gradient-doping structure, we study the carrier concentration distribution in such structural epilayers after the MBE growth with electrochemical capacitance-voltage (ECV) profiling. Besides, the inherent mechanism of electron transport in gradient-doping transmission-mode GaAs photocathodes is analyzed in detail.

2. Experiment

The gradient-doping transmission-mode GaAs sample was grown on the high quality p-type GaAs (100) oriented substrate with Be doping by using an

*Project supported by the National Natural Science Foundation of China (Grant Nos 60678043 and 60801036).

†Corresponding author. E-mail: bkchang@mail.njust.edu.cn

Applied EPI GEN-II MBE system. During the growth process, the epitaxial layers composed of buffer-layer, active-layer, window-layer and protection-layer were grown by MBE according to priority. The active-layer of the sample is a gradient-doping structure which is divided into four sections with the Be doping concentration ranging from 1×10^{19} cm^{-3} to 1×10^{18} cm^{-3}, while the Be doping concentration of the GaAlAs window-layer is designed as 1×10^{19} cm^{-3} to reduce the back interface recombination probability between the active-layer and window-layer. The overall structure with the thickness and doping levels of the epilayers is shown in Fig.1.

protection-layer	0.1 μm GaAs (no-doping)
window-layer	1 μm GaAlAs 1.0×10^{19} cm^{-3}
active-layer	0.5 μm GaAs 1.0×10^{19} cm^{-3}
	0.5 μm GaAs 5.0×10^{18} cm^{-3}
	0.5 μm GaAs 2.5×10^{18} cm^{-3}
	0.5 μm GaAs 1.0×10^{18} cm^{-3}
buffer-layer	1 μm GaAlAs (no-doping)
high-quality p-type GaAs (100) substrate	

Fig.1. Doping structure of the gradient-doping transmission-mode GaAs photocathode grown by MBE.

As a result of the multiple epilayers structure of the gradient-doping transmission-mode GaAs photocathodes, we used the Bio-Rad ECV system to measure the carrier vertical distribution in each layer. The ECV technique can expediently determine the carrier distribution condition and band offsets at isotype heterointerface of the multiple-layer semiconductor materials.[10,11]

After the ECV measurement, the cutted sample was made into the cathode module with a glass/Si_3N_4/GaAlAs/GaAs structure by etching the substrate, buffer-layer and protection-layer. Following that, the sample surface of 18 mm in diameter was activated to NEA state in the ultrahigh vacuum chamber ($\leq10^{-9}$ Pa) using the improved activation technique,[12,13] in which cesium source was kept continuously and oxygen source was opened and closed periodically. After the "high-low temperature" two-step activation, the cathode module was sealed into a third generation image-intensifier tube, in which the microchannel plate (MCP) and fluorescence screen were removed, and then the spectral response of the sealed image tube was measured by the spectral response measurement instrument.[14]

3. Results and discussion

With the aid of the Bio-Rad ECV system, the carrier concentration vertical distribution versus depth in Be-doped GaAs/GaAlAs epilayers, namely the active-layer and the window-layer, was measured after the MBE growth. As shown in Fig.2, we can get a clear picture of the inner carrier concentration distribution, just as the gradient-doping structure of the designed sample. Nevertheless, the actual carrier concentration measured by ECV represents the active dopant concentration, that is to say, parts of Be atoms become the acceptor impurities contributing to the carrier concentration, while there are still some other neutral Be atoms remaining inactive in GaAs and GaAlAs which do not supply carriers to the materials, thus the measured carrier concentration is somewhat lower than the doping concentration. The measured carrier concentration in the GaAs active-layer ranges from 3×10^{18} cm^{-3} to 5×10^{17} cm^{-3} which is composed of four stages, while that in GaAlAs window-layer is no more than 2×10^{18} cm^{-3}, which results in an abrupt interface with the GaAs active-layer.

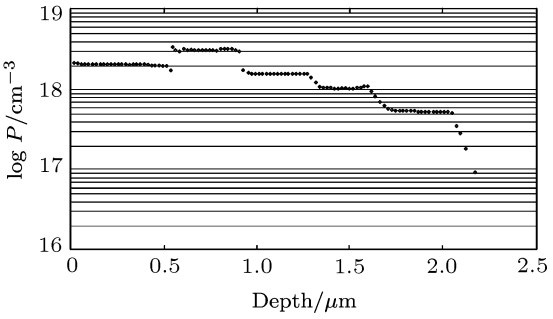


Fig.2. Vertical distribution of carrier concentration in GaAs/GaAlAs epilayers after the MBE growth measured by ECV profiling.

In addition, the measured spectral response curve of this gradient-doping transmission-mode GaAs photocathode is shown in Fig.3. The obtained integral sensitivity has achieved 1420 μA/lm with a high and flat response ranging from 560 nm to 880 nm, which is higher than the traditional uniform-doping

GaAs photocathodes.[15] The result confirms that the gradient-doping GaAs photocathodes can be very useful to the practical device application.

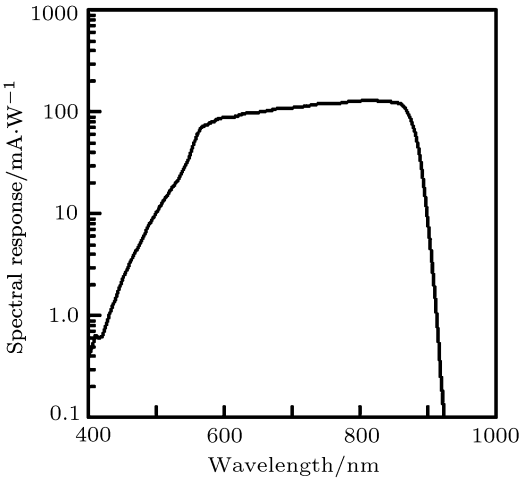


Fig.3. Spectral response curve of the gradient-doping transmission-mode GaAs photocathode.

In order to make clear what influences the gradient-doping structure, this problem has brought on the performance of transmission-mode GaAs photocathodes, we should carry on an investigation into the intrinsic band structure of the gradient-doping transmission-mode GaAs photocathodes at first. As shown in Fig.4, the doping concentration is distributed gradiently from high to low in the bulk-to-surface GaAs active-layer. This gradient-doping structure can result in many downward band bending regions, which help form built-in electric fields to facilitate photoexcited electrons movement toward surface.

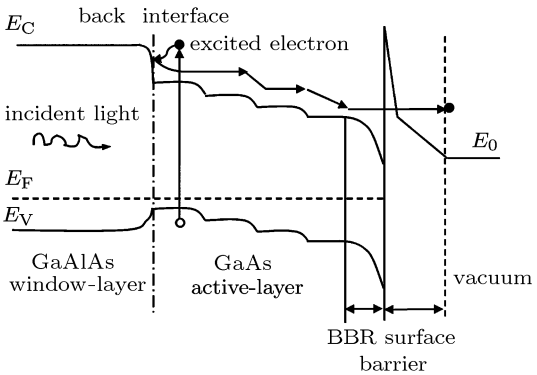


Fig.4. Band structure diagram of gradient-doping transmission-mode GaAs photocathodes. E_C is the conduction band minimum, E_V is the valence band maximum, E_F is the Fermi level, E_0 is the vacuum level, and BBR is the surface band-bending region.

There is a band-bending region (BBR) at each interface formed by the Fermi-level leveling effect between two different doping concentration sections. Suppose that the actual carrier concentrations of the two adjacent sections are N_{A1} and N_{A2} respectively, where $N_{A1} > N_{A2}$, the band-bending energy qV_D due to the carrier concentration discrepancy is given by

$$\begin{aligned} qV_D &= E_{F2} - E_{F1} \\ &= \left(E_V + k_0 T \ln \frac{N_V}{N_{A2}}\right) - \left(E_V + k_0 T \ln \frac{N_V}{N_{A1}}\right) \\ &= k_0 T \ln \frac{N_{A1}}{N_{A2}}, \end{aligned} \tag{1}$$

where E_{F1} is the Fermi level of section 1, E_{F2} is the Fermi level of section 2, k_0 is Boltzmann constant, T is absolute temperature, E_V is the valence band maximum, and N_V is the valence band density of states of GaAs.

Using Eq.(1), we have obtained the BBE values of the gradient-doping GaAs, which are composed of four sections after the MBE growth, and are listed in Table 1. In the GaAs active-layer, section 1 corresponds to the layer with the highest carrier concentration while section 4 corresponds to the layer with the lowest carrier concentration.

Table 1. Band-bending energy of gradient-doping GaAs layer after the MBE growth.

band-bending energy/meV			total band-bending energy/meV
section1∼ section 2	section2∼ section 3	section3∼ section 4	
14.7	13.7	17.9	46.3

According to Table 1, we find that there is a BBE at each interface between two sections of different concentration in gradient-doping GaAs photocathodes, which is useful to make the photoexcited electron acceleratively move toward surface by way of diffusion and directional drift, because of the built-in electric fields. Therefore, the electron diffusion length in gradient-doping GaAs photocathodes can be larger than that in uniform-doping ones.

Although the gradient carrier concentration is helpful to the photoexcited electron transport, the adverse carrier concentration discrepancy between GaAs and GaAlAs is unexpected which has resulted in an abrupt back interface to capture and recombine parts of the photoexcited electrons. As a result of the large band gap of GaAlAs, the band edge offsets between the GaAlAs and GaAs form a potential barrier that pushes photoexcited electrons from the wide gap side (GaAlAs) to the narrow gap side (GaAs) in this heterostructure. As a matter of fact, the GaAs/GaAlAs interface acts as an electron potential barrier $\Delta E_{\rm C}$ by reflecting electrons back toward the vacuum interface when the photoexcited electrons diffuse toward back interface.

The electron potential barrier $\Delta E_{\rm C}$ can be obtained by analysis of the band edge offsets between GaAlAs and GaAs through the following equation

$$\Delta E_{\rm C} = \Delta E_{\rm g} - \Delta E_{\rm V} = \Delta E_{\rm g} - [(E_{\rm F} - E_{\rm V1}) - (E_{\rm F} - E_{\rm V2})], \tag{2}$$

where $E_{\rm F}$ is the unity Fermi level for GaAlAs and GaAs by the Fermi-level leveling effect, $E_{\rm V1}$ and $E_{\rm V2}$ are the valence band maxima of GaAlAs and GaAs, respectively. The band bending structure of the GaAs/GaAlAs heterojunction could be determined by the discontinuities in the conduction bands $\Delta E_{\rm C}$ and in the valence bands $\Delta E_{\rm V}$, which are also the commonly called band offsets.

In Eq.(2), $\Delta E_{\rm g}$ indicates the difference in band gap energy between the wide gap energy $E_{\rm g1}$ of GaAlAs and the narrow gap energy $E_{\rm g2}$ of GaAs. It is noted that we only take account of the Γ direct band gap energy $E_{\rm g}^{\Gamma}$ on account of the electronic easy transition to direct conduction band minimum. As for GaAs, $E_{\rm g2}$ is equal to 1.424 eV at room temperature, while for GaAlAs, $E_{\rm g1}$ depends on the Al content x and is given by[16]

$$E_{\rm g1} = \begin{cases} 1.424 + 1.247x, & (0 \le x \le 0.45), \\ 1.424 + 1.247x + 1.147(x - 0.45)^2, & (0.45 \le x \le 1.0). \end{cases} \tag{3}$$

In this work, the Al content x is designed as 0.63, and then $E_{\rm g1}$ for GaAlAs at room temperature is equal to 2.247 eV. In addition, the values of $E_{\rm F} - E_{\rm V1}$ and $E_{\rm F} - E_{\rm V2}$ can be calculated through the carrier concentration P measured by ECV profiling, and the calculative equations are given by

$$E_{\rm F} - E_{\rm V} = k_0 T \ln(N_{\rm V}/P), \tag{4}$$

$$N_{\rm V} = 2.5 \times 10^{19} (m_{\rm p}/m_0)^{3/2} (T/300)^{3/2}, \tag{5}$$

where $N_{\rm V}$ is the effective density of states for the valence band of the p-type GaAs/GaAlAs epilayers, and $m_{\rm p}/m_0$ is the ratio of the effective mass to the free-electron mass. For GaAs, $m_{\rm p}/m_0$ is equal to 0.48, while for GaAlAs, $m_{\rm p}/m_0$ depends on the Al content x and is given by[16]

$$m_{\rm p} = (0.48 + 0.31x) m_0. \tag{6}$$

Using Eqs.(2)–(6), we can obtain the value of $\Delta E_{\rm C}$ (in eV) at 300 K as a function of the Al content x and the carrier concentration ratio P_2/P_1, the presented equation is expressed by

$$\Delta E_{\rm C} = \begin{cases} 1.247x - \dfrac{300 k_0 \ln\{(P_2/P_1)[1 + (0.31x/0.48)^{3/2}]\}}{1.6 \times 10^{-19}}, & (0 \le x \le 0.45), \\ 1.247x + 1.147(x - 0.45)^2 - \dfrac{300 k_0 \ln\{(P_2/P_1)[1 + (0.31x/0.48)^{3/2}]\}}{1.6 \times 10^{-19}}, & (0.45 \le x \le 1.0). \end{cases} \tag{7}$$

According to Eq.(7), when the Al content x of GaAlAs layer is 0.63, the obtained values of ΔE_C are plotted against the carrier concentration ratio P_2/P_1 in Fig.5. It is clear that the smaller the carrier concentration in GaAs than that in GaAlAs is, the greater value ΔE_C can achieve for reflecting more high-energy photoexcited electrons back to vacuum interface. As shown in Fig.6, with the interface potential barrier at GaAs/GaAlAs heterointerface ascending, it is possible to make less high-energy excited electrons get across the interface potential barrier, which will improve the short-wave response for the transmission-mode photocathodes. For this sample grown by MBE, the electron potential barrier ΔE_C is calculated to be 0.799 eV using the carrier concentration measured by ECV profiling, therefore, the amount of photoexcited electrons of energy larger than 2.223 eV (wavelength≤560 nm) will be decreased in terms of back interface recombination. Therefore, it is necessary to elevate the back interface electron potential barrier in order to increase more reflected high-energy photoexcited electrons.

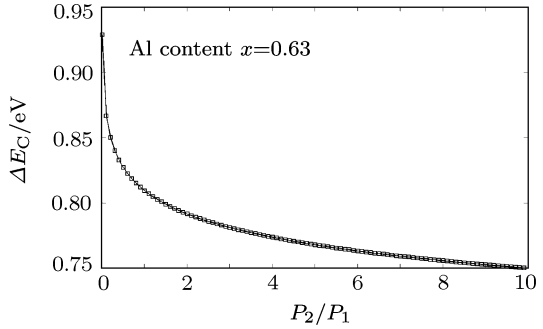


Fig.5. Relation between electron potential barrier ΔE_C and the carrier concentration ratio P_2/P_1 for GaAs/GaAlAs heterointerface. The P_1 and P_2 represent the carrier concentration in GaAlAs and adjacent GaAs, respectively.

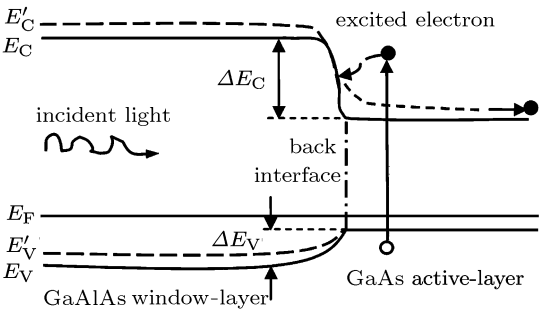


Fig.6. Variation in band bending structure of the GaAs/GaAlAs heterointerface. The E_C, E_V and E_F marked by the solid line represent band structure of the original sample grown by MBE, while E'_C and E'_V marked by the dashed line represent band structure assuming that the carrier concentration discrepancy of back interface becomes smaller.

4. Conclusion

In this paper, we have applied the gradient-doping structure to the transmission-mode GaAs photocathode, and the integral sensitivity of the sealed image tube has achieved 1420 μA/lm which is higher than the traditional uniform-doping one. In order to know the inner actual gradient-doping structure, the carrier concentration distribution of the gradient-doping transmission-mode GaAs photocathode has been investigated after MBE growth by the use of ECV profiling. With the MBE growth, we get an ideal gradient-doping structure. Besides, we have calculated the BBE in the gradient-doping GaAs active-layer, and the total BBE is 46.3 meV which helps improve the photoexcited electrons movement toward surface for the thin epilayer. On the other hand, it is found that when the Al content in GaAlAs is constant, the worse carrier concentration discrepancy between GaAs and GaAlAs will decrease the amount of high-energy photoelectrons which are unable to be reflected by the lower back interface electron potential barrier, therefore, we should heighten the Be doping level in GaAlAs to reduce the disadvantageous factor in back interface recombination for good photoemission in the future work.

Acknowledgements

The authors would like to thank Zeng Yi-Ping of Institute of Semiconductors, Chinese Academy of Sciences for supplying the transmission-mode GaAs sample, and Shi Feng *et al* of Xi'an Institute of Applied Optics for the assistance in the experiment.

References

[1] Zhou L W, Li Y, Zhang Z Q, Monastyrski M A and Schelev M Y 2005 *Acta Phys. Sin.* **54** 3591 (in Chinese)

[2] Zou J J, Chang B K and Yang Z 2007 *Acta Phys. Sin.* **56** 2992 (in Chinese)

[3] Liu Z, Sun Y, Peterson S and Pianetta P 2008 *Appl. Phys.*

Lett. **92** 241107
[4] Narayanan A A, Fisher D G, Erickson L P and O'Clock G D 1984 *J. Appl. Phys.* **56** 1886
[5] Bourree L E, Chasse D R, Thamban P L S and Glosser R 2003 *Proc. SPIE* **4796** 11
[6] Ilegems M 1977 *J. Appl. Phys.* **48** 1278
[7] Spicer W E and Herrera-Gómez A 1993 *Proc. SPIE* **2022** 18
[8] Zou J J and Chang B K 2006 *Opt. Eng.* **45** 054001
[9] Yang Z, Chang B K, Zou J J, Qiao J L, Gao P, Zeng Y P and Li H 2007 *Appl. Opt.* **46** 7035
[10] Okumura H, Misawa S, Yoshida S and Gonda S 1985 *Appl. Phys. Lett.* **46** 377
[11] Udhayasankar M, Kumar J and Ramasamy P 2004 *J. Cryst. Growth* **268** 389
[12] Ruan C J 2003 *Chin. Phys.* **12** 483
[13] Li Q, Hao L and Pang W N 2008 *Acta Phys. Sin.* **57** 172 (in Chinese)
[14] Zong Z Y, Qian Y S and Chang B K 2001 *Proc. SPIE* **4580** 623
[15] Xu J T 2000 *J. Appl. Opt.* **21** 5 (in Chinese)
[16] Casey H C and Jr. 1978 *J. Appl. Phys.* **49** 3684